Author(s):	Koho, Tiia; Ihalainen, Teemu; Stark, Marie; Uusi-Kerttula, Hanni; Wieneke, Ralph; Rahikainen, Rolle; Blazevic, Vesna; Marjomäki, Varpu; Tampé, Robert; Kulomaa, Markku; Hytönen, Vesa
Title:	His-tagged norovirus-like particles: A versatile platform for cellular delivery and surface display
Year:	2015
Journal Title:	European Journal of Pharmaceutics and Biopharmaceutics
Vol and number:	96 : 15
Pages:	22-31
ISSN:	1873-3441
Discipline:	Biomedicine
School /Other Unit:	BioMediTech; School of Medicine
Item Type:	Journal Article
Language:	en
DOI:	http://dx.doi.org/10.1016/j.ejpb.2015.07.002
URN:	URN:NBN:fi:uta-201508062214

His-tagged Norovirus-like Particles: A Versatile Platform for Cellular Delivery and Surface Display

Tiia Koho[1], Teemu O. Ihalainen[1], Marie Stark[2], Hanni Uusi-Kerttula[3], Ralph Wieneke[4], Rolle Rahikainen[1], Vesna Blazevic[3], Varpu Marjomäki[2], Robert Tampé[4], Markku S. Kulomaa[1], Vesa P. Hytönen[1,5,]*

[1]BioMediTech, University of Tampere, Biokatu 6, FI-33520 Tampere, Finland.
[2]Department of Biological and Environmental Science/Nanoscience Center, Survontie 9, FI- 40500 Jyväskylä, Finland
[3]Vaccine Research Center, Medical School, University of Tampere, Biokatu 10, FI-33520 Tampere, Finland
[4]Institute of Biochemistry, Biocenter, Goethe-University Frankfurt, Max-von-Laue-Strasse 9, D-60438 Frankfurt am Main, Germany
[5]Fimlab Laboratories, Biokatu 4, FI-33520 Tampere, Finland.

*Email: Vesa P. Hytönen (Vesa.Hytonen@uta.fi)
BioMediTech, University of Tampere, Biokatu 6, FI-33520 Tampere, Finland.

Keywords: virus-like particle (VLP), bioconjugation, molecular display, cell entry peptide, targeting, drug delivery

Abstract

In addition to vaccines, noninfectious virus-like particles (VLPs) that mimic the viral capsid show an attractive possibility of presenting immunogenic epitopes or targeting molecules on their surface. Here, functionalization of norovirus-derived VLPs by simple non-covalent conjugation of various molecules is shown. By using the affinity between a surface-exposed polyhistidine-tag and multivalent *tris*-nitrilotriacetic acid (*tris*NTA), fluorescent dye molecules and streptavidin-biotin conjugated to *tris*NTA are displayed on the VLPs to demonstrate the use of these VLPs as easily modifiable nanocarriers as well as a versatile vaccine platform. The VLPs are able to enter and deliver surface-displayed fluorescent dye into HEK293T cells via a surface-attached cell internalization peptide (VSV-G). The ease of manufacturing, the robust structure of these VLPs, and the straightforward conjugation provide a technology, which can be adapted to various applications in biomedicine.

Introduction

Virus-like particles (VLPs) are nanoscale, multisubunit protein structures with an identical or highly similar overall structure as the corresponding native viruses. Thus, these particles have the ability to mimic many of viral features such as competence to self-assemble into an organized icosahedral or helical shell with a symmetric and highly repetitive structure, and to bind and enter cells using appropriate surface receptors. Moreover, due to their size and highly repetitive symmetric structure, VLPs are capable of inducing strong B and T cell-mediated immune responses. These particles are, however, incapable of causing infection because they are devoid of the viral genetic material and catalytic proteins needed in the viral replication [1,2]. Due to these inherent advantages, VLPs have become a widely accepted platform in prophylactic vaccine technology. In fact, certain VLP-based vaccines are currently on the market (Recombivax HB, Engerix-B, Gardasil and Cervarix), and many other VLP-based products are at different stages of clinical studies. Furthermore, VLPs offer the intriguing possibility of producing chimeric VLPs in which one or multiple antigens are genetically fused to viral structural proteins or conjugated chemically to the VLPs [3].

In addition to vaccines, VLPs also exhibit great potential in a number of other applications, such as novel therapeutics. In the field of gene and immune therapy, VLP-based tools have been developed by modulating VLP packaging, display, and/or targeting (reviewed extensively, for example, in [3-7]). Furthermore, VLPs even show promise as new biological nanomaterials [8-12]. As a nanocarrier platform, VLPs offer the advantages of morphological uniformity, biocompatibility, the capacity to potentiate the immune response, and easy functionalization. A variety of VLPs are suitable for chemical or genetic modifications of their inner cavities and outer surfaces, which enables the attachment of not only covalently bound drug molecules or antigens but also various cell or tumor targeting ligands [1,3,4].

During the past decade, VLPs have been mainly used as vaccines. In addition, there is an increasing number of reports in which chimeric VLPs from different viral origins were prepared by either

genetic fusion or chemical coupling of epitope peptides or other molecules to the inner or outer surfaces of the VLPs (reviewed, for example, in [13]). However, in all of these cases, the display was achieved by genetic fusion of the protein fragment and the VLP sequence or by covalent chemical linkage to the reactive residues of the VLP surface. The production of new genetically fused VLPs is a laborious and slow undertaking that, even without encountering problems, can take several weeks to accomplish. Moreover, there are limitations to the size and nature of epitopes that can be genetically inserted into VLPs without endangering the VLP self-assembly process. In chemical conjugation of molecules to a preassembled VLP, the size and structure of the attached molecule is not limited by the correct folding requirements of the components, or restricted to an attachment of only peptide molecules [14].

Although the potential of several icosahedral VLPs tailored with genetic and chemical conjugation in biomedical applications has been studied in detail (reviewed recently in [13]), such modification procedures have not been established for norovirus (NoV) VLPs so far. However, the presentation of foreign antigens attached to surface loops of NoV capsid-derived subviral P particles has been reported [15]. Noroviruses are the leading cause of acute epidemic gastroenteritis across all age groups worldwide, causing symptoms such as nausea, vomiting, abdominal cramps, and diarrhea. Although NoV gastroenteritis is generally mild and short-lasting, severe illness and complications can occur in the elderly, in children, and in immunocompromised individuals [16,17]. Recombinant expression of the major capsid protein VP1 results in VLPs that are morphologically similar to the infective virion [18], and the crystal structure of the capsid is known (PDB ID:1IHM) [19], which is essential for the establishment of modification procedures. The approximately 40-nm-sized capsid consists of 180 VP1 capsid proteins organized into 90 dimers. NoV VLPs can be robustly expressed in insect cells, in transgenic plants, and in yeast. For example, a highly efficient (>0.6 g/l) secreted production of NoV VLPs from *Pichia pastoris* was described recently [20]. Also, NoV

VLP-based vaccines are under active development. The first human VLP-based NoV vaccine developed by Takeda Pharmaceuticals is currently being evaluated in clinical efficacy trials [21].

In this report, a nanocarrier platform based on modified VLPs and non-covalent chemical conjugation is described. The VLPs were derived from norovirus (NoV VLPs) and modified by adding a C-terminal polyhistidine tag, which projected out of the VLP surface (Figure 1A). The norovirus genotype GII-4 utilized in this study has been previously expressed as unmodified VLP by us [22] and others [23]. The polyhistidine tag was first utilized in VLP purification and later employed to attach different cargo molecules non-covalently on the VLP surface via *tris*-nitrilotriacetic acid (*tris*NTA) adaptors. The surface-modified NoV VLP nanocarriers were characterized in detail and implemented in delivering a conjugated fluorescent dye as a model molecule into human cells (Figure 1B). This technology provides a universal nanoparticle tool for the adaptation of vaccine delivery or targeting, for increasing and fine-tuning vaccine immunogenicity or bioavailability via a displayable molecule, and for use as surface building blocks. The ease of particle manufacturing, the robust structure of NoV VLPs, and the straightforward conjugation makes this platform highly suitable for multiple purposes.

Figure 1. Schematic presentation of the concept of VLP display and ligand-mediated VLP delivery. (A) Surface presentation of the NoV capsid (PDB ID: 1IHM), with C-terminal residues highlighted in yellow cube and the C-terminal Cα residues highlighted with red spheres, in addition to the chemical structure of the *tris*NTA-(Alexa488) used in the study. (B) The NoV VLP nanocarriers were used to deliver surface-conjugated fluorescent dye into human cells with the help of surface-conjugated VSV-G (vesicular stomatitis virus glycoprotein G) peptide.

Material and Methods

Virus-like particle production and purification: A C-terminal polyhistidine tag was added to norovirus (GII.4) capsid sequence [22] by polymerase chain reaction (PCR) using the primers GII-

4for: 5'-CAC AGC TAG CAT GAA GAT GGC GTC GAA TGA C-3' and GII-4rev: 5'-CTC TGC ATG CTT AGT GGT GGT GGT GGT GGT GTA ATG CAC GTC TAC G-3'. The resulting PCR product was cloned under the pPH promoter in the baculovirus transfer vector pFastBac™ Dual (Invitrogen, Carlsbad, CA) via introduced restriction sites (Nhe I and SphI) to produce fully his-tagged VLPs. For partially his-tagged chimeric VLPs, a native NoV capsid sequence (without the C-terminal his-tag) was cloned under the other promoter (p10) in the same transfer vector using the EcoRI and BamHI restriction sites. The recombinant baculoviruses were generated according to the instructions for the Bac-to-Bac® Baculovirus Expression System (Invitrogen). A native NoV VLP described previously [24] was used as a control in several experiments.

The VLPs were expressed in baculovirus-transformed *Spodoptera frugiperda* insect cells (Sf9; Invitrogen) and harvested 5-6 days post-infection. After clarification by centrifugation (10 000 × g at 4°C for 20 min), NaCl and imidazole were added to the clarified supernatant at final concentrations of 200-700 mM and 20 mM, respectively. The VLPs were purified using a 5-ml HisTrap FF Crude column (GE Healthcare, Uppsala, Sweden). A buffer containing 20 mM NaH_2PO_4, 500 mM NaCl, and 20 mM imidazole (pH 7.4) was used as the running buffer, and running buffer containing imidazole (500 mM) was used as the elution buffer. Column-bound VLPs were eluted using a linear gradient (target: 60% elution buffer, gradient length: 30 ml). A flow rate of 2 ml/min was used throughout the chromatographic purification. The VLP-containing fractions were pooled, dialyzed, and stored at 4°C until further use. Total protein concentrations were analyzed using the Pierce® BCA Protein Assay Kit (Thermo Scientific, Rockford, IL).

Virus-like particle characterization: For assessment of the total protein content, the NoV VLP samples were run on a 12% SDS-PAGE gel and subsequently visualized using Oriole™ Fluorescent Gel Stain (Bio-Rad, Hercules, CA). The VLPs' primary morphology and size were characterized in 3% uranyl acetate-stained samples by JEM-1400 TEM (JEOL, Tokyo, Japan). The hydrodynamic

diameter of the VLPs calculated as the averages of six consecutive measurements, each consisting of 16×10-s readings measured at 25°C using the Zetasizer Nano ZS DLS instrument (Malvern Instruments Ltd., Worcestershire, UK) and predetermined viscosity and refractive index values. VLP integrity upon heating was analyzed using the Zetasizer Nano ZS instrument as well. The hydrodynamic diameter was determined using three 10×10-s datasets collected at 25°C in 20 mM NaH_2PO_4, 500 mM NaCl (pH 7.4). The sample was further subjected to stepwise heating. Starting at 25°C, the sample was heated in 5°C intervals and equilibrated for 5 min at each temperature before analysis. The samples were heated to 90°C, after which the samples were cooled back to 25°C. The denaturation was found to be irreversible.

The antigenic properties of the VLPs and their binding to their putative receptors were analyzed by an enzyme-linked immunosorbent assay (ELISA) and a histo-blood group antigen (HBGA) assay, respectively, as described previously [22]. The engineered VLPs and the native NoV VLP control were used as antigens in the ELISA, and were examined using 12 NoV-positive human sera. The synthetic HBGAs examined in this study were H type 1 and H type 3. A representative result is reported.

Synthesis of the nitrilotriacetic acid compounds: Synthesis of *tris*NTA-VSV-G: NTA-SGGG-YTDDIEMNRLGK-NH_2 was synthesized by Fmoc solid-phase chemistry using L-amino acids and Fmoc-Rink-Amide MBHA resin [25,26]. All reaction steps were performed under microwave-irradiation using the Liberty 1 (CEM) and standard coupling protocols for microwave-assisted solid phase synthesis were used throughout the synthesis. Coupling reactions were performed using HBTU, diisopropylethylamine and the corresponding Fmoc- amino acids, and 20% piperidine was employed for Fmoc-deprotection. O*t*Bu-protected carboxy-NTA was coupled to the peptide using COMU. Cleavage was achieved using 95% TFA and 5% scavengers (phenol, TIPS, water, and EDT; 1.25% of each) as a cleavage cocktail for 3 h following lyophilization and purification by RP-

HPLC (PerfectSil™ C18 column 250×4.6 mm, 300 ODS, 5 µm; MZ-Analysentechnik, Mainz, Germany) using a gradient from water to 35% methanol, both containing 0.1% TFA. MALDI-TOF-MS: m/z 2788.4 (calculated for $(M + H)^+$: 2785.2 $C_{113}H_{176}N_{30}O_{50}S$). The purified product was solubilized in 10 mM HEPES (pH 7.0) and a 20-fold molar excess of $NiCl_2$ was added. After 2 h at room temperature, Ni-loaded *tris*NTA-VSV-G was isolated by size exclusion chromatography (PD Midi Trap G-10, GE Healthcare, Buckinghamshire, UK).

Synthesis of *tris*NTA-Alexa488 and *tris*NTA-biotin: A total of 1.2 equivalents of NHS-activated Alexa488 and 20 eq. DIPEA were added to a solution of amine-functionalized *tris*NTA in DMF (25 mM) [27]. The solution was stirred for 24 h at room temperature in the dark and subsequently purified via RP-C18-HPLC using a gradient from 5% ACN to 15% ACN, with the buffers containing 0.1% TFA. The purified product was lyophilized and solubilized in 10 mM HEPES (pH 7.0). A 15-fold molar excess of $NiCl_2$ was added and the reaction mixture was incubated for 2 h at room temperature. Ni-loaded *tris*NTA-Alexa488 was isolated by anion exchange chromatography (1 ml HiTrapTM Q HP, GE Healthcare). After a washing step with 10 ml of 50 µM EDTA (10 mM HEPES buffer, pH 7.0), Ni-loaded *tris*NTA-Alexa488 was eluted using a gradient from 0 to 1 M NaCl (10 mM HEPES, pH 7.0). *tris*NTA-biotin was prepared by using NHS-activated biotin and the purification as well as the Ni-loading step were conducted as described above.

Conjugation experiments: Streptavidin (SA) was attached to the surface of engineered NoV VLPs using the *tris*NTA-biotin conjugate that bound to a polyhistidine tag. SA was first attached to the *tris*NTA-biotin conjugate using simple equimolar mixing of SA (tetramer concentration of 16 µM) and *tris*NTA-biotin with $NiSO_4$ (100 mM) in PBS buffer. After 3 h incubation using a roller mixer, the excess $NiSO_4$ was removed by dialysis against 20 mM NaH_2PO_4, 500 mM NaCl (pH 7.4). A 50-fold molar excess of *tris*NTA-biotin-SA conjugate relative to his-tagged VLPs was used. The resulting increase in the hydrodynamic diameter of the VLP-SA complexes was detected at 22°C

using dynamic light scattering (DLS). SA alone with his-tagged VLPs was used as a negative control.

To analyze the binding capacity of his-tagged VLPs, *tris*NTA-Alexa488 (0.4 µM) was incubated with VLPs (0.2 µM) in 20 mM NaH_2PO_4, 500 mM NaCl (pH 7.4) at room temperature for 2 h. The excess dye-conjugate was removed by ultrafiltration using an Amicon® Ultra-0.5 mL centrifugal device (MWCO 30K; MerckMillipore, Darmstadt, Germany). The samples were analyzed using UV/Vis spectroscopy, and labeling ratios per VLP were determined.

Fluorescence correlation spectroscopy (FCS) was conducted by using a Zeiss LSM 780 confocal fluorescence microscope equipped with a Plan Apochromat 63x/1.2 water immersion objective. The argon laser intensity was adjusted to 1.5% of the maximum of the 488-nm laser line. The pinhole was set to 1 Airy -unit. The samples were diluted in 50 mM NaH_2PO_4, 1 M NaCl (pH 7.2) and studied using a Lab-Tek II™ 8-well chamber coverglass (Nunc, Roskilde, Denmark). Buffer alone gave low count rate of 0.398 kHz, without any signs of fluorescence correlation. The FCS data was analyzed by using the following parameters: geometric correction 1, structural parameter 5, and triplet state relaxation time 2 µs. After *tris*NTA-Alexa488 conjugate (8 nM) alone was measured and 10×10-s or 100×1-s datasets were collected, a 1-component model was applied to the data. Individual measurements with a diffusion time over 300 µs were omitted from the analysis (accounting for less than 10% of the data). The analysis resulted in an average diffusion time of 77.8 µs and a count rate of 1.52 kHz per dye. The diffusion time for the VLPs (1974.8 µs) was determined from a solution containing *tris*NTA-Alexa488-conjugated All-His-VLPs prepared as described above. The titration experiment was performed by using a solution of 8 nM *tris*NTA-Alexa488, to which VLPs were added gradually, and the amount of the second component (1974.8 µs) was determined after each addition of the VLPs. Imidazole displacement experiments were performed by mixing 5 mM or 20 mM imidazole into a solution containing different VLPs (subunit concentration of 135 nM) conjugated to *tris*NTA-Alexa488 (8 nM).

Virus-like particle delivery experiments: Transduction of HEK293T cells with VLPs consisting of surface-displayed *tris*NTA-Alexa488 and *tris*NTA-SGGG-VSV-G-peptide conjugates was performed by plating 5×10^4 HEK293T cells per well overnight on 35 mm glass bottom Petri dishes (MatTek Corporation, Ashland, MA). The next day, the culture medium was changed and supplemented with VLPs (112 nM) displaying *tris*NTA-Alexa488 and *tris*NTA-SGGG-VSV-G-peptide conjugates (conjugated using 2× and 5× molar excess over the capsid protein, respectively) or VLPs displaying only *tris*NTA-Alexa488 conjugate, or with only PBS (as a negative control). The cells were exposed to samples or controls for 3 h, after which the cells were washed three times with PBS and fixed with 4% PFA. The actin filaments in the cell cytoskeleton were stained with AlexaFluor®568 Phalloidin stain (LifeTechnologies, Eugene, OR). The samples were imaged with a Zeiss LSM 780 confocal fluorescence microscope using a Plan Apochromat 63x/1.4 oil immersion objective (Carl Zeiss, Jena, Germany). The experiment was performed two times with two parallel samples.

The average cell intensities in images acquired with a 488-nm excitation laser were analyzed by using ImageJ version 1.49m. Briefly, the raw 3D image stacks saved in .CZI format were imported as 8-bit grayscale images and projected into 2D images by using the maximum intensity projection of each image. The average fluorescence intensities of the cells were then measured by selecting each cell with the freehand tool and by using the "Multi measure" command for analyzing the selected areas. A total of 11-21 cells were analyzed per sample. The average background intensities of the images were measured from a 30×30-µm square outside the cell areas and subtracted from the average intensity values of the analyzed cells. Statistical significance was determined by unpaired two-tailed *t*-test.

Ni-NTA particle binding assay: Availability of the polyhistidine sequences on the VLPs were studied by incubating 100 µg/ml solution of the cHis-VLPs with Ni-NTA beads (Protino® Ni-NTA

agarose; Macherey-Nagel-GMbH & Co., Düren, Germany) in 50 mM NaPO4, 100 mM NaCl (pH 7.2). After 120 min incubation at 4°C, the beads were collected by centrifugation and a sample was taken from the supernatant (Unbound, Supplementary Figure S3). The pellet was resuspended to the same buffer and pelleted again to release loosely bound VLPs (Wash, Supplementary Figure S3). Finally, a sample was taken from the washed Ni-NTA beads (Bound, Supplementary Figure S3) and all the samples were analyzed with SDS-PAGE followed by Coomassie staining.

Results and Discussion

The chimeric NoV VLPs were generated by infecting insect cells with recombinant baculoviruses encoding only the C-terminally histidine (his)-tagged norovirus capsid gene (producing fully his-tagged VLPs, All-cHis-VLPs) or both the C-terminally his-tagged and the wild-type NoV capsid gene (producing partially his-tagged VLPs, cHis-VLPs). Subsequent purification of the VLPs using immobilized metal ion affinity chromatography (IMAC) resulted in homogenous particles of the expected size and morphology, as confirmed by transmission electron microscopy (TEM) and dynamic light scattering (DLS). The yield after chromatographic purification was 3.0 mg/l cell culture for cHis-VLP and 1.5 mg/l for All-cHis-VLP. TEM revealed that the engineered VLPs were monodisperse, uniform in size (diameter of approximately 40 nm) and morphologically indistinguishable from native NoV VLPs (Figure 2A). The DLS-measured mean hydrodynamic diameters of native VLPs (VLPs), cHis-VLPs, and All-cHis-VLPs were 44±1, 42±1, and 42±1 nm, respectively (Figure 2B). The numbers were calculated from the volume distribution-weighted intensity and are expressed as the mean±standard deviation of six independent readings. DLS analysis revealed only one particle population in each sample with a low polydispersity index (PdI) value. The PdI, which describes the width of the intensity-weighted mean diameter distribution measured by DLS, was 0.062, 0.098, and 0.026 for VLPs, cHis-VLPs, and All-cHis-VLPs, respectively. For reference, a sample is typically referred to as monodisperse if the PdI value is below 0.1, whereas values greater than 0.7 indicate a very broad size distribution and thereby a very

polydisperse sample [28]. Thus, the results suggest that the samples contained monodisperse and pure VLPs and demonstrate that addition of the C-terminal histidine tag did not interfere with protein folding or VLP assembly. Moreover, the added histidine tags most likely projected out of the VLP surface, or otherwise the VLPs could not have been purified and concentrated by IMAC. The binding efficiency of the cHis-VLPs was evaluated by mixing 0.1 mg/ml purified VLP with IMAC resin. After incubation, the resin was collected by centrifugation and washed. The bound VLPs were then assayed using SDS-PAGE (Supplementary Figure S3). Majority of the VLPs was found to remain bound to resin, indicating tight binding. The heat stability remained also unaltered, since no differences in the aggregation temperature (60°C) were observed between the engineered VLPs and native VLP control when the VLP samples were heated from 25°C to 90°C (Figure 2C).

Figure 2. Biophysical characterization of the engineered VLPs. (A) TEM images of native NoV VLPs and of partially and fully polyhistidine-tagged NoV VLPs. Scale bar, 50 nm. (B) Hydrodynamic diameters of the respective VLPs measured by DLS and presented as a size distribution by volume. The mean size of the VLPs varied from approximately 42 nm for histidine-tagged VLPs to 44 nm for native VLPs. The mean measurement of six independent readings is expressed for each VLP sample. (C) Analysis of the aggregation temperature. Gradual heating of the VLP samples from 25°C to 90°C resulted in aggregation at 60°C, irrespective of the particle type.

The purified VLP samples were found to be essentially free from contaminating proteins, when their total protein content was assessed by running the samples on an Oriole-stained SDS-PAGE gel (Figure 3A). The purity was estimated to be over 95%. The double-band pattern within the SDS-PAGE gel (Figure 3A) is known to be associated with the 34-residue fragment missing from the N-terminus of a fraction of capsid proteins [22], and this phenomenon has been observed in several earlier studies [18,29-31].

The effect of NoV VLP surface engineering on VLP antigenicity and putative receptor-binding capability were analyzed using ELISA and histo-blood group antigen (HBGA) assays, respectively.

The engineered VLPs were found to retain their antigenic ability despite the surface-expressed histidine tags (Figure 3B), as shown by the fact that antigen recognition of both types of engineered VLPs by human NoV-positive sera was high and comparable to that of the native NoV VLPs [22] [24] that were used as a control. The binding activity of the engineered VLPs to their putative receptors and host-susceptibility factors was also unaltered and comparable to that of the control, as demonstrated by comparing their binding activities to synthetic oligosaccharides representing H type 1 and H type 3 HBGAs (Figure 3C). Together these results demonstrate that similar to the native NoV VLPs already tested in preclinical trials [32], both of these engineered NoV VLP constructs are applicable as vaccine candidates against NoV. The advantage of these engineered VLPs is that the surface-displayed polyhistidine tag allows both direct manipulation of the VLP surface and implementation of an easy and scalable IMAC-based purification protocol that does not include polyethylene glycol (PEG) precipitation. By masking the particle's surface, PEG may cause problems in downstream applications, interfere with ligand binding, and suppress the desired immune responses [33].

Figure 3. Sample purity and antigenic assessment of the engineered VLPs. (A) Analysis of Oriole-stained SDS-PAGE gels showed that the engineered VLPs were efficiently purified, without contaminating proteins, by IMAC. Lane 1: molecular weight marker; lane 2: chromatography input sample for the cHis-VLPs; lanes 3-5: cHis-VLP-containing elution samples; lane 6: molecular weight marker; lane 7: chromatography input sample for the All-cHis-VLPs; lanes 8-10: All-cHis-VLP-containing elution samples. (B) No differences in immunoreactivity with human NoV-positive sera were detected between the engineered and the native VLPs. Data from a representative serum sample from 12 analyzed sera is shown. (C) The binding of engineered VLPs to synthetic HBGAs, which act as putative receptors and host-susceptibility factors for NoV, was comparable to that of native VLPs.

Next, the surface-integrated polyhistidine tags were utilized to demonstrate molecule display on VLPs by using *tris*NTA-biotin adaptors to non-covalently attach SA to the surface of the polyhistidine-tagged VLPs. *tris*NTA binds polyhistidine tags via coordinating metal ions with high

affinity and stability [27] and has been shown to be nontoxic to cells [25]. The attachment of *tris*NTA-biotin-SA complexes to VLPs was detected as an increase in the hydrodynamic diameter of the VLP-SA complexes, as measured by DLS (Figure 4). The hydrodynamic diameters of the cHis-VLPs and control (cHis-VLPs with SA), measured based on the volume distribution (100% in all measurements) were 42±1 nm and 43±1 nm (PdIs: 0.098 and 0.053), respectively, whereas when SA was conjugated to the cHis-VLP surface via the *tris*NTA-biotin adaptor, the diameter increased to 52±1 nm (PdI: 0.113). A similar outcome occurred when SA was conjugated to All-cHis-VLPs. The hydrodynamic diameter of the All-cHis-VLP-SA complexes increased to 49±1 nm (PdI: 0.110) from 45±1 nm for All-cHis-VLPs alone and 45±1 nm for the control (PdIs: 0.079 and 0.037, respectively). The increase in the diameter of the VLP forms is in agreement with the diameter increase calculated for the SA tetramer (approximately 5 nm) accompanied by the *tris*NTA adaptor and thus demonstrates that proteins can be attached to the VLP surface without causing disturbance to the particle structure. A similar set-up was demonstrated by Chackerian et al. [34], although they first covalently biotinylated surface-exposed lysine residues on papillomavirus-like particles and then utilized the SA-biotin interaction to attach self-antigens via SA fusion proteins. Others utilized the interaction between NTA and hexahistidine to encapsulate fluorescent dyes inside human polyomavirus JC VLPs as a model for a pH-dependent drug release system [35].

Figure 4. SA conjugation. Attaching SA onto the surface of the cHis-VLPs (A) and the All-cHis-VLPs (B) increased the hydrodynamic diameter of the particles. VLP+SA (dark gray) represents a control experiment, in which streptavidin was added to the VLP sample without the *tris*NTA-biotin adaptor. The hydrodynamic diameters were measured by DLS and are presented here as an intensity distribution.

To estimate the number of available binding sites for *tris*NTA-conjugated molecules on the VLPs, the particles were labeled using Alexa488 fluorescent dye-conjugated *tris*NTA. The two his-tagged VLP forms were labeled with a 2-fold molar excess of Alexa488 conjugate (4 µM). After removal of the excess dye by ultrafiltration, the obtained labeled particles were studied by UV/Vis spectroscopy and labeling efficiencies of 68 and 74 dye molecules per VLP were determined for cHis-VLPs and All-cHis-VLPs, respectively (data not shown).

The *tris*NTA-Alexa488-conjugated VLPs were then subjected to fluorescence correlation spectroscopy (FCS) to assay the number of the fluorescent conjugates per VLP and to study the binding properties more thoroughly. In accordance with the UV/Vis results, FCS revealed particles with high intensity and only a negligible background signal, indicating attachment of the conjugate with high affinity. Based on the fluorescence intensity measured for the *tris*NTA-Alexa488 conjugate alone, a count rate of 1.52 kHz per dye was estimated. Respective peak intensities obtained as an average of the ten most intense peaks were 131.2±28.9 kHz and 246.8±45.5 kHz for *tris*NTA-Alexa-conjugated cHis-VLPs and All-cHis-VLPs (data not shown). Therefore, based on the count rate measured for the *tris*NTA-Alexa488 conjugate alone and assuming that its fluorescence intensity in solution is identical to that of the VLP-attached conjugate, it was estimated that each cHis-VLP carried 86±19 dye molecules on its surface, whereas 162±30 dye molecules were carried by each All-cHis-VLP. Furthermore, a nearly identical diffusion time of approximately 2000 µs was consistently observed for both types of VLPs, indicating that the solutions were monodisperse after conjugation. This finding was supported by the fact that the data could be fitted with a single component model. The same diffusion time was observed when short (1-s) measurements corresponding to the intense peaks were analyzed, suggesting that the peaks indeed represented individual VLPs. The determined 2-ms diffusion time is reasonable for particles with a diameter of approximately 40 nm [36].

To further characterize the interaction between his-tagged VLPs and nickel-coordinated *tris*NTA-Alexa488, a titration experiment was conducted, in which the VLPs were added to a solution containing the fluorescent conjugate at a concentration of 8 nM. In the absence of VLPs, a stable fluorescence signal with average intensity of 24 kHz was observed (Figure 5A). When cHis-VLPs or All-cHis-VLPs were added, fluorescence intensity fluctuation increased significantly (Figure 5C and D, respectively), indicating the accumulation of the fluorescent conjugate on the particles. Native VLPs showed only minor (unspecific) accumulation of the dye (Figure 5B). By fitting a 2-component model with predefined diffusion times (77.8 µs for the dye and 1974.8 µs for the VLPs) to the obtained data, the amount of the fluorescence signal associated with the VLPs as a function of the VLP concentration could be determined (Figure 5E). Reflecting the relative amount of available binding sites on the engineered VLPs, strong binding of a high number of *tris*NTA-Alexa488 was observed for All-cHis-VLPs, whereas cHis-VLPs showed a slightly lower level of binding to the dye. Minor accumulation of the fluorescent dye was observed also for native VLPs; however, addition of 5 mM imidazole completely abolished the interaction between native VLPs and *tris*NTA-Alexa488 (Figure 5F). In contrast, for both types of his-tagged VLPs only a moderate decrease in particle complexation was observed by 5 mM imidazole. For All-cHis-VLPs, the addition of 5 mM imidazole caused a decrease in complexation from 80% to 50%, whereas for cHis-VLPs a decrease from 40% to 20% was observed (Figure 5E and F). The fluorescent dye was completely released from all of the VLPs by 20 mM imidazole (data not shown), confirming the specificity of the assay. FCS analysis indicates that 50% of the dye was bound to All-cHis-VLPs at a VLP subunit concentration of less than 30 nM (Figure 5E). In comparison, cHis-VLPs show 50%-binding at a subunit concentration of ~130 nM, which is in line with the fact that not all of the subunits are histidine-tagged. These findings suggest that the binding of *tris*NTA-Alexa to histidine-tagged VLPs is tight with a K_d of 10-50 nM. Earlier, a K_d of 20 nM has been determined

for the polyhistidine - *tris*NTA interaction [27] and our findings are thus well in line with the previous data.

Figure 5. Attachment of the *tris*NTA-Alexa488 conjugate to the engineered VLPs. (A-D) Count rates of different VLPs over time analyzed by FCS. (A) *tris*NTA-Alexa488 showed a constant fluorescence signal. (B) The addition of native VLPs at a subunit concentration of 15 nM caused no significant changes in fluorescence intensity fluctuation, whereas (C) cHis-VLPs and (D) All-cHis-VLPs led to the appearance of high-intensity peaks. (E) Percentage of large particles as a function of the VLP subunit concentration derived from 2-component correlation analysis with predetermined diffusion times. (F) Percentage of large particles in a mixture of *tris*NTA-Alexa488 (8 nM) and VLPs (subunit concentration of 135 nM). Imidazole (5 mM) completely abolished the interaction between native VLPs and the *tris*NTA-Alexa488 conjugate, whereas only a moderate decrease in the fraction of large particles was observed in the case of histidine-tagged VLPs.

Drug delivery has become a key stone in therapeutic development, as new potent therapeutic molecules are often restricted by a lack of cellular uptake and insufficient capability to reach targets. In the present study, a VSV-G protein fragment was attached onto a VLP surface to enable its entry into cells. VSV-G is commonly used in biomedical research to pseudotype viral vectors due to its ability to transduce a broad range of mammalian cell types with genes of interest without being transported into endosomal vesicles [37,38]. To demonstrate the effectiveness of engineered VLPs in delivering foreign molecules into cells, human embryonic kidney (HEK293T) cells were exposed to All-cHis-VLPs non-covalently decorated with *tris*NTA-Alexa488 fluorescent dye. Because NoV is inherently incapable of infecting cultured cells, VSV-G peptides were attached to the VLP surface using *tris*NTA adaptors to enable them enter into cells. As shown in Figure 6, the delivery of Alexa488 into HEK293T cells was only observed when cells were exposed to VLPs displaying both Alexa488 and VSV-G conjugates. By contrast, there was no detectable fluorescence signal observed in the cells exposed to VLPs displaying Alexa488 conjugate in the absence of VSV-G conjugate, nor was there any signal in the untreated control. When the fluorescence intensities from 11-21 cells per sample were analyzed as maximum intensity projections of the cell area, the cells treated with Alexa488- and VSV-G-displaying VLPs had an average intensity of 8.3±1.2, whereas

clearly less was observed for the control sample (Alexa488-VLPs), with an intensity of 2.3±0.2. The difference was statistically significant ($p<0.001$), and similar results were observed in two independent experiments. Taken together, the VSV-G conjugated to the VLPs enabled the VLPs to transduce cells and carry the surface-conjugated Alexa488 dye along. This experiment also demonstrated that these NoV VLPs could be functionalized to versatile nanocarriers by simple non-covalent conjugation of different molecules. Surface functionalization with some other relevant targeting peptide would allow targeting of these nanocarriers into specific cell types and delivering perhaps therapeutic peptides along.

Figure 6. VLP-mediated fluorescent dye delivery into cultured cells. HEK293T cells were treated for 3 h with PBS (A), with *tris*NTA-Alexa488-conjugated VLPs (B), or with *tris*NTA-Alexa488- and *tris*NTA-VSV-G peptide-conjugated VLPs (C). The images are middle sections from the confocal z-axis. Scale bar 10 µm.

This experimental set-up can be considered challenging, as the VSV-G peptide transduces cells as a trimer [39] and there was no control over the exact location of conjugation as to enter three adjacent peptides near each other. This configuration therefore differs from the traditional method of pseudotyping, in which the VSV-G is inherently integrated into the VLP or virus envelope through co-transfection of expression vectors. In the current study, the control VLPs, which only displayed the *tris*NTA-Alexa488 conjugate, demonstrated that transduction was dependent of the VSV-G peptide. An analogous idea for circumventing the problem of uncultivable NoV was presented by Ma and Li [40], who showed that the whole capsid protein of NoV could be expressed on recombinant VSV to form NoV VLPs that were attenuated in cultured mammalian cells as well as in mice.

Although it is known that chemically synthesized peptides are capable of eliciting antibodies, the peptides by themselves present low immunogenicity and a high level of clearance. Immunogenicity

and bioavailability can be increased by conjugating or fusing the peptides to carrier proteins, thereby extending their lifetime and presenting them in a manner in which they will be better recognized by the immune system [41,42]. Therefore, VLPs that mimic the viral capsid show an attractive possibility of presenting immunogenic epitopes on their surface, allowing the use of these chimeric constructs for vaccination and in gene and drug therapy. Because norovirus infections are harmful and even life-threatening for certain subjected groups, immunization against NoV VLPs can be considered beneficial "side-effect". Moreover, it has been found, that existing NoV VLP antibodies do not block the immunization with another NoV VLP [43]. Therefore, despite the high level of pre-existing NoV antibodies [43,44], the use of NoV VLPs as a carrier might not be impaired by them. Applications for these engineered VLPs include the creation of novel vaccines presenting unique immunological content on their surface; steering or enhancing the immune response; targeting specific cells; and encapsidation or display of different molecules, from nucleotides, genes, peptides and proteins to therapeutic drugs and inorganic nanomaterials [13,45].

Conclusions

As a summary, a systematic analysis of the functional effects of introducing artificial modulatory sites onto the NoV VLP surface is provided in this study. We also provide proof of principle for a fast "click-and-exchange" technology for modulating the VLP surface simply by replacing the conjugated molecule that binds to the polyhistidine tags on the VLP surface. Surface display is therefore achieved without laborious genetic fusion of the displayable molecule and capsid gene or permanent chemical coupling to a preformed VLP. If needed, the displayable molecule can be separated from the VLP with mild treatment with imidazole, after which the VLP is fully reusable. The concept is widely applicable to variety of molecules. The NoV VLP surface could be decorated, for example, with therapeutic peptides that enhance or modulate the immune system or with epitopes, small proteins, DNA, reporter tags for tracing vaccine delivery, or targeting molecules, just to name a few. Moreover, we present here two types of polyhistidine-tagged VLP forms,

differing by the number of conjugation sites that they bear, allowing accommodation of larger complexes and modulation of the number of conjugates on the surface. If administered to humans, an immune response may also be elicited against the actual NoV VLP carrier. However, this event can only be considered as a beneficial side effect because it may, at the same time, protect the individual from the harmful NoV infections to come. In conclusion, the histidine-tagged NoV VLPs described in this study offer a robust and versatile tool for the needs of nanobiotechnology and biomedical sciences.

Acknowledgements

The authors thank Ulla Kiiskinen and Niklas Kähkönen for assistance with insect cell cultures and preparation of reagents and buffers, and the Biocenter Finland for infrastructure support. We thank Latifeh Azizi and Dr. Juha Määttä for the help in chromatography. The work was supported by grants from the Academy of Finland (136288 and 273192 to V.P.H, 261285 and 272288 to M.S.K), and from The National Doctoral Programme in Informational and Structural Biology (ISB). The German Research Foundation (Ta157/9 - SPP 1623) and the Cluster of Excellence Macromolecular Complexes supported this work.

References

[1] A. Zeltins, Construction and characterization of virus-like particles: a review, Mol. Biotechnol. 53 (2013) 92-107.

[2] I. Vorackova, P. Ulbrich, W.E. Diehl, T. Ruml, Engineered retroviral virus-like particles for receptor targeting, Arch. Virol. 159 (2014) 677-688.

[3] N. Kushnir, S.J. Streatfield, V. Yusibov, Virus-like particles as a highly efficient vaccine platform: diversity of targets and production systems and advances in clinical development, Vaccine. 31 (2012) 58-83.

[4] Y. Ma, R.J. Nolte, J.J. Cornelissen, Virus-based nanocarriers for drug delivery, Adv. Drug Deliv. Rev. 64 (2012) 811-825.

[5] R.L. Garcea, L. Gissmann, Virus-like particles as vaccines and vessels for the delivery of small molecules, Curr. Opin. Biotechnol. 15 (2004) 513-517.

[6] S.D. Xiang, K. Scalzo-Inguanti, G. Minigo, A. Park, C.L. Hardy, M. Plebanski, Promising particle-based vaccines in cancer therapy, Expert Rev. Vaccines. 7 (2008) 1103-1119.

[7] G.T. Jennings, M.F. Bachmann, Immunodrugs: therapeutic VLP-based vaccines for chronic diseases, Annu. Rev. Pharmacol. Toxicol. 49 (2009) 303-326.

[8] Q. Wang, T. Lin, L. Tang, J.E. Johnson, M.G. Finn, Icosahedral virus particles as addressable nanoscale building blocks, Angew. Chem. Int. Ed Engl. 41 (2002) 459-462.

[9] C. Mao, D.J. Solis, B.D. Reiss, S.T. Kottmann, R.Y. Sweeney, A. Hayhurst, G. Georgiou, B. Iverson, A.M. Belcher, Virus-based toolkit for the directed synthesis of magnetic and semiconducting nanowires, Science. 303 (2004) 213-217.

[10] L.A. Lee, Z. Niu, Q. Wang, Viruses and virus-like protein assemblies - Chemically programmable nanoscale building blocks, Nano Research. 2 (2009) 349-364.

[11] Z. Liu, J. Qiao, Z. Niu, Q. Wang, Natural supramolecular building blocks: from virus coat proteins to viral nanoparticles, Chem. Soc. Rev. 41 (2012) 6178-6194.

[12] A.D. Brown, L. Naves, X. Wang, R. Ghodssi, J.N. Culver, Carboxylate-directed in vivo assembly of virus-like nanorods and tubes for the display of functional peptides and residues, Biomacromolecules. 14 (2013) 3123-3129.

[13] P. Pushko, P. Pumpens, E. Grens, Development of virus-like particle technology from small highly symmetric to large complex virus-like particle structures, Intervirology. 56 (2013) 141-165.

[14] G.T. Jennings, M.F. Bachmann, The coming of age of virus-like particle vaccines, Biol. Chem. 389 (2008) 521-536.

[15] M. Tan, M. Xia, P. Huang, L. Wang, W. Zhong, M. McNeal, C. Wei, X. Jiang, Norovirus P Particle as a Platform for Antigen Presentation, Procedia in Vaccinology. 4 (2011) 19-26.

[16] R.I. Glass, U.D. Parashar, M.K. Estes, Norovirus gastroenteritis. N. Engl. J. Med. 361 (2009) 1776-1785.

[17] M.M. Patel, A.J. Hall, J. Vinje, U.D. Parashar, Noroviruses: a comprehensive review. J. Clin. Virol. 44 (2009) 1-8.

[18] X. Jiang, M. Wang, D.Y. Graham, M.K. Estes, Expression, self-assembly, and antigenicity of the Norwalk virus capsid protein. J. Virol. 66 (1992) 6527-6532.

[19] B.V. Prasad, M.E. Hardy, T. Dokland, J. Bella, M.G. Rossmann, M.K. Estes, X-ray crystallographic structure of the Norwalk virus capsid, Science. 286 (1999) 287-290.

[20] J. Tome-Amat, L. Fleischer, S.A. Parker, C.L. Bardliving, C.A. Batt, Secreted production of assembled Norovirus virus-like particles from Pichia pastoris, Microb. Cell. Fact. 13 (2014) 134-014-0134-z.

[21] K. Debbink, L.C. Lindesmith, R.S. Baric, The state of norovirus vaccines, Clin. Infect. Dis. 58 (2014) 1746-1752.

[22] T. Koho, L. Huhti, V. Blazevic, K. Nurminen, S.J. Butcher, P. Laurinmäki, N. Kalkkinen, G. Rönnholm, T. Vesikari, V.P. Hytönen, M.S. Kulomaa, Production and characterization of virus-like particles and the P domain protein of GII.4 norovirus, J. Virol. Methods. 179 (2012) 1-7.

[23] D.J. Allen, R. Noad, D. Samuel, J.J. Gray, P. Roy, M. Iturriza-Gomara, Characterisation of a GII-4 norovirus variant-specific surface-exposed site involved in antibody binding, Virol. J. 6 (2009) 150-422X-6-150.

[24] T. Koho, T. Mäntylä, P. Laurinmäki, L. Huhti, S.J. Butcher, T. Vesikari, M.S. Kulomaa, V.P. Hytönen, Purification of norovirus-like particles (VLPs) by ion exchange chromatography, J. Virol. Methods. 181 (2012) 6-11.

[25] R. Wieneke, N. Laboria, M. Rajan, A. Kollmannsperger, F. Natale, M.C. Cardoso, R. Tampe, Live-cell targeting of his-tagged proteins by multivalent N-nitrilotriacetic acid carrier complexes, J. Am. Chem. Soc. 136 (2014) 13975-13978.

[26] N. Laboria, R. Wieneke, R. Tampe, Control of nanomolar interaction and in situ assembly of proteins in four dimensions by light, Angew. Chem. Int. Ed Engl. 52 (2013) 848-853.

[27] S. Lata, A. Reichel, R. Brock, R. Tampe, J. Piehler, High-affinity adaptors for switchable recognition of histidine-tagged proteins, J. Am. Chem. Soc. 127 (2005) 10205-10215.

[28] Malvern Instruments, Dynamic Light Scattering. Common Terms Defined. Inform White Paper. (2011).

[29] A. Bertolotti-Ciarlet, S.E. Crawford, A.M. Hutson, M.K. Estes, The 3' end of Norwalk virus mRNA contains determinants that regulate the expression and stability of the viral capsid protein VP1: a novel function for the VP2 protein. J. Virol. 77 (2003) 11603-11615.

[30] M. Tan, W. Zhong, D. Song, S. Thornton, X. Jiang, E. coli-expressed recombinant norovirus capsid proteins maintain authentic antigenicity and receptor binding capability. J. Med. Virol. 74 (2004) 641-649.

[31] L.J. White, M.E. Hardy, M.K. Estes, Biochemical characterization of a smaller form of recombinant Norwalk virus capsids assembled in insect cells. J. Virol. 71 (1997) 8066-8072.

[32] K. Tamminen, S. Lappalainen, L. Huhti, T. Vesikari, V. Blazevic, Trivalent combination vaccine induces broad heterologous immune responses to norovirus and rotavirus in mice, PLOS ONE. 8 (2013) e70409.

[33] M.D. Scott, K.L. Murad, Cellular camouflage: fooling the immune system with polymers, Curr. Pharm. Des. 4 (1998) 423-438.

[34] B. Chackerian, D.R. Lowy, J.T. Schiller, Conjugation of a self-antigen to papillomavirus-like particles allows for efficient induction of protective autoantibodies, J. Clin. Invest. 108 (2001) 415-423.

[35] N. Ohtake, K. Niikura, T. Suzuki, K. Nagakawa, S. Mikuni, Y. Matsuo, M. Kinjo, H. Sawa, K. Ijiro, Low pH-triggered model drug molecule release from virus-like particles, Chembiochem. 11 (2010) 959-962.

[36] T. Gao, C.D. Blanchette, W. He, F. Bourguet, S. Ly, F. Katzen, W.A. Kudlicki, P.T. Henderson, T.A. Laurence, T. Huser, M.A. Coleman, Characterizing diffusion dynamics of a membrane protein associated with nanolipoproteins using fluorescence correlation spectroscopy, Protein Science. 20 (2011) 437-447.

[37] A.A. Mironov, G.V. Beznoussenko, P. Nicoziani, O. Martella, A. Trucco, H.S. Kweon, D. Di Giandomenico, R.S. Polishchuk, A. Fusella, P. Lupetti, E.G. Berger, W.J. Geerts, A.J. Koster, K.N. Burger, A. Luini, Small cargo proteins and large aggregates can traverse the Golgi by a common mechanism without leaving the lumen of cisternae, J. Cell Biol. 155 (2001) 1225-1238.

[38] J. Cronin, X.Y. Zhang, J. Reiser, Altering the tropism of lentiviral vectors through pseudotyping, Curr. Gene Ther. 5 (2005) 387-398.

[39] X. Sun, S.L. Roth, M.A. Bialecki, G.R. Whittaker, Internalization and fusion mechanism of vesicular stomatitis virus and related rhabdoviruses, Future Virol. 5 (2010) 85-96.

[40] Y. Ma, J. Li, Vesicular stomatitis virus as a vector to deliver virus-like particles of human norovirus: a new vaccine candidate against an important noncultivable virus, J. Virol. 85 (2011) 2942-2952.

[41] M.F. Bachmann, G.T. Jennings, Vaccine delivery: a matter of size, geometry, kinetics and molecular patterns, Nat. Rev. Immunol. 10 (2010) 787-796.

[42] W. Liu, Y.H. Chen, High epitope density in a single protein molecule significantly enhances antigenicity as well as immunogenicity: a novel strategy for modern vaccine development and a preliminary investigation about B cell discrimination of monomeric proteins, Eur. J. Immunol. 35 (2005) 505-514.

[43] K. Tamminen, L. Huhti, T. Vesikari, V. Blazevic, Pre-existing immunity to norovirus GII-4 virus-like particles does not impair de novo immune responses to norovirus GII-12 genotype, Viral Immunol. 26 (2013) 167-170.

[44] X. Jiang, N. Wilton, W.M. Zhong, T. Farkas, P.W. Huang, E. Barrett, M. Guerrero, G. Ruiz-Palacios, K.Y. Green, J. Green, A.D. Hale, M.K. Estes, L.K. Pickering, D.O. Matson, Diagnosis of human caliciviruses by use of enzyme immunoassays, J. Infect. Dis. 181 Suppl 2 (2000) S349-59.

[45] A. Palucha, A. Loniewska, S. Satheshkumar, A.M. Boguszewska-Chachulska, M. Umashankar, M. Milner, A.L. Haenni, H.S. Savithri, Virus-like particles: models for assembly studies and foreign epitope carriers, Prog. Nucleic Acid Res. Mol. Biol. 80 (2005) 135-168.

Figure 1

Click here to download high resolution image

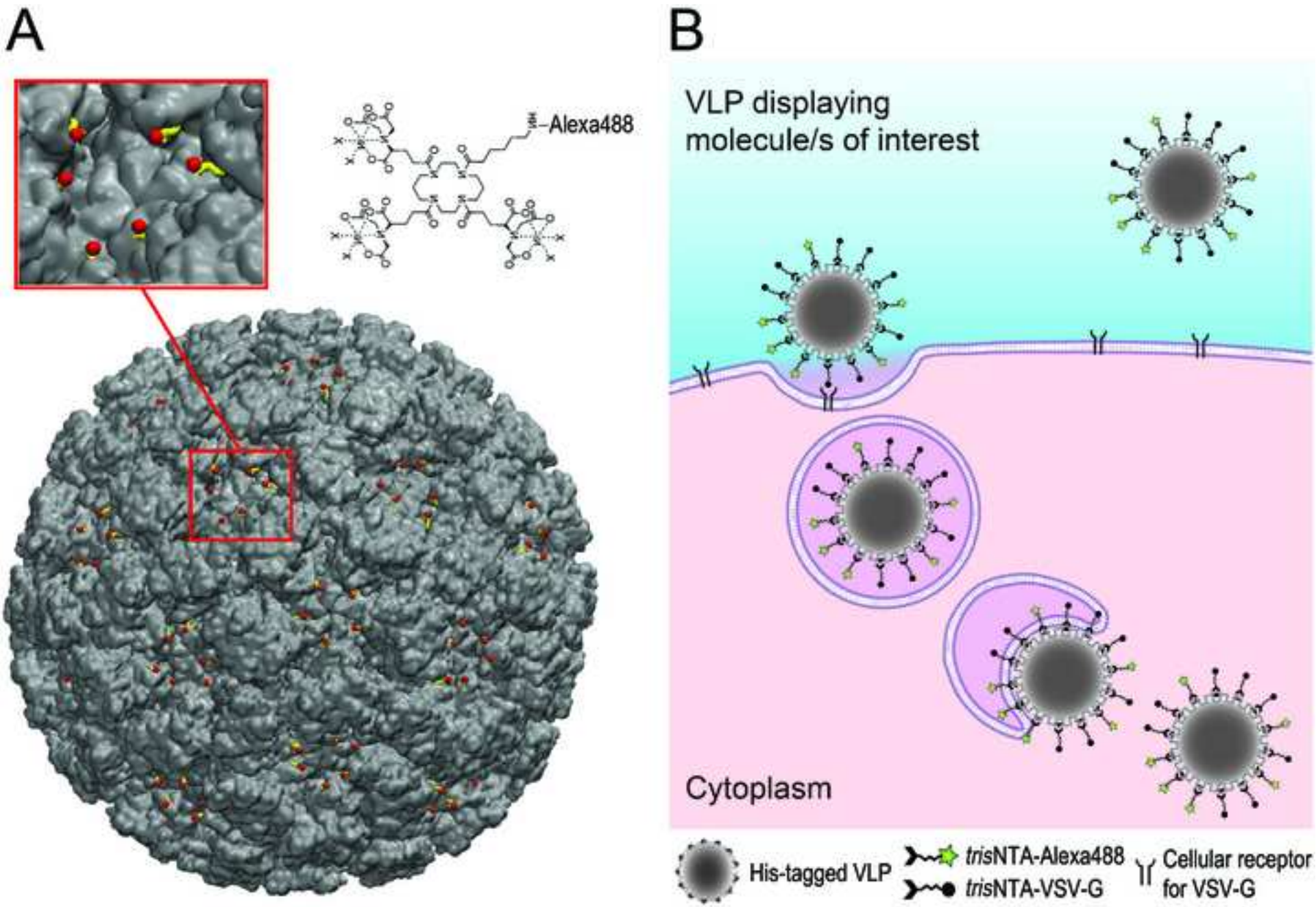

Figure 2

Click here to download high resolution image

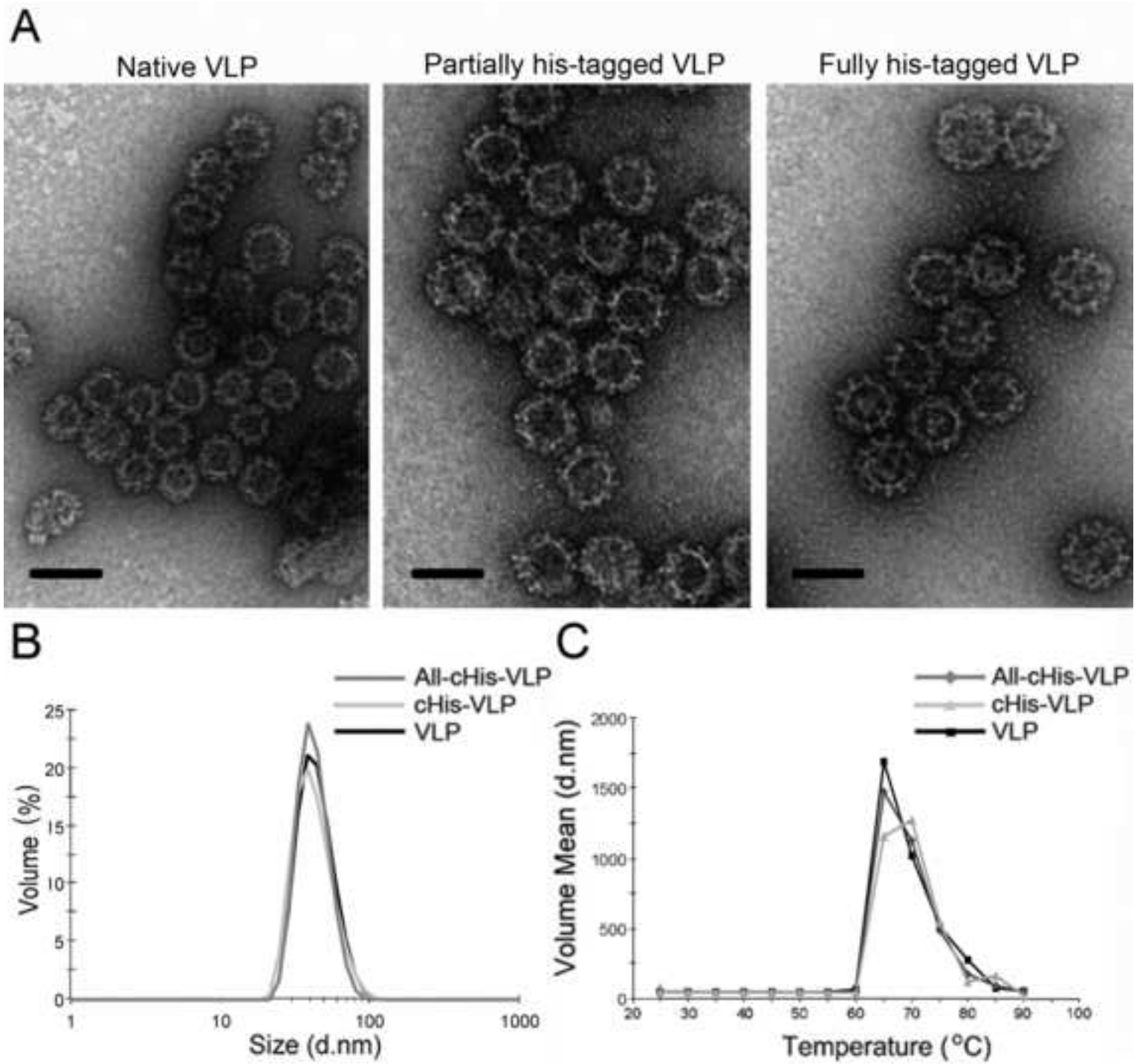

Figure 3

Click here to download high resolution image

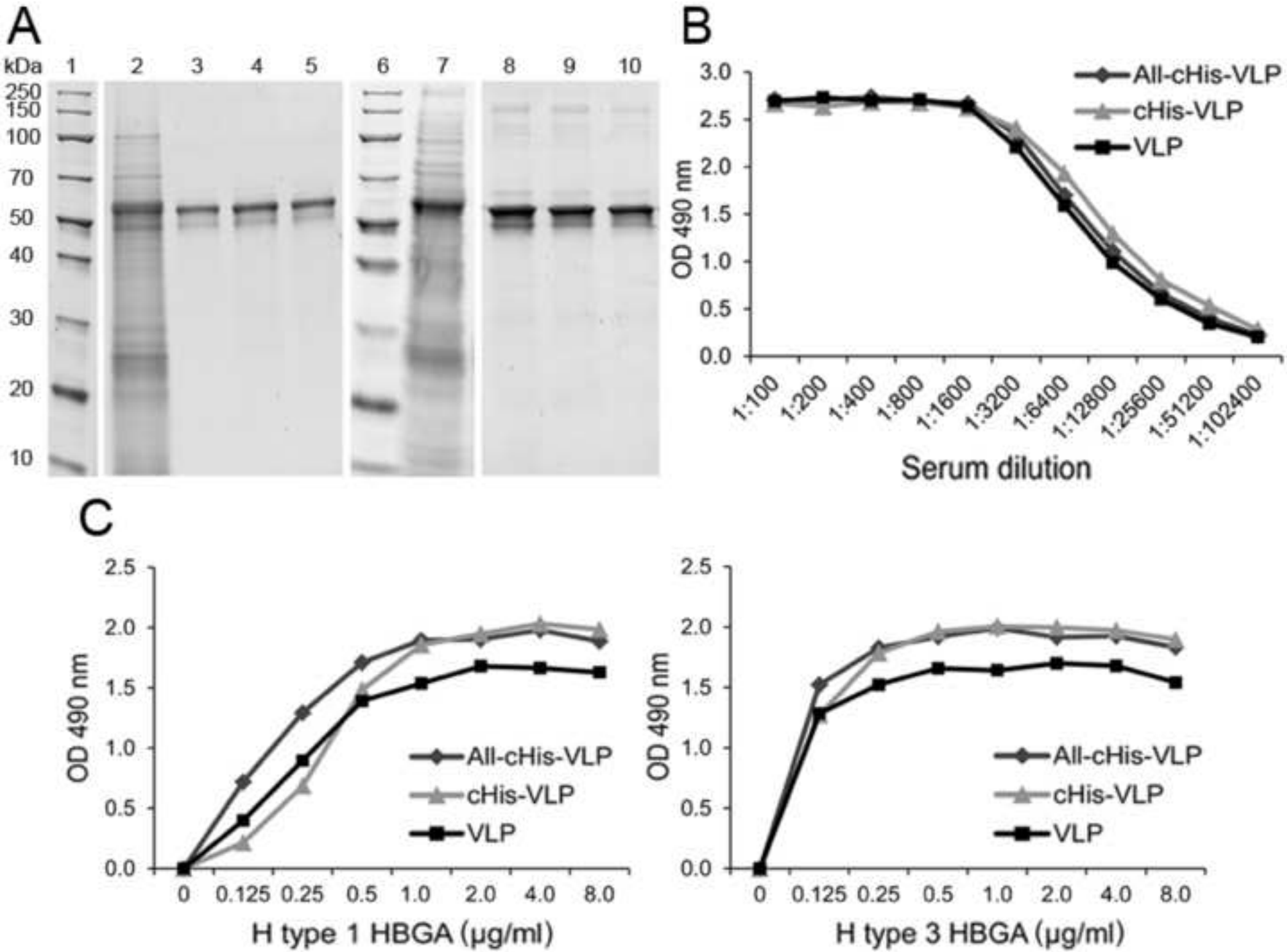

Figure 4

Click here to download high resolution image

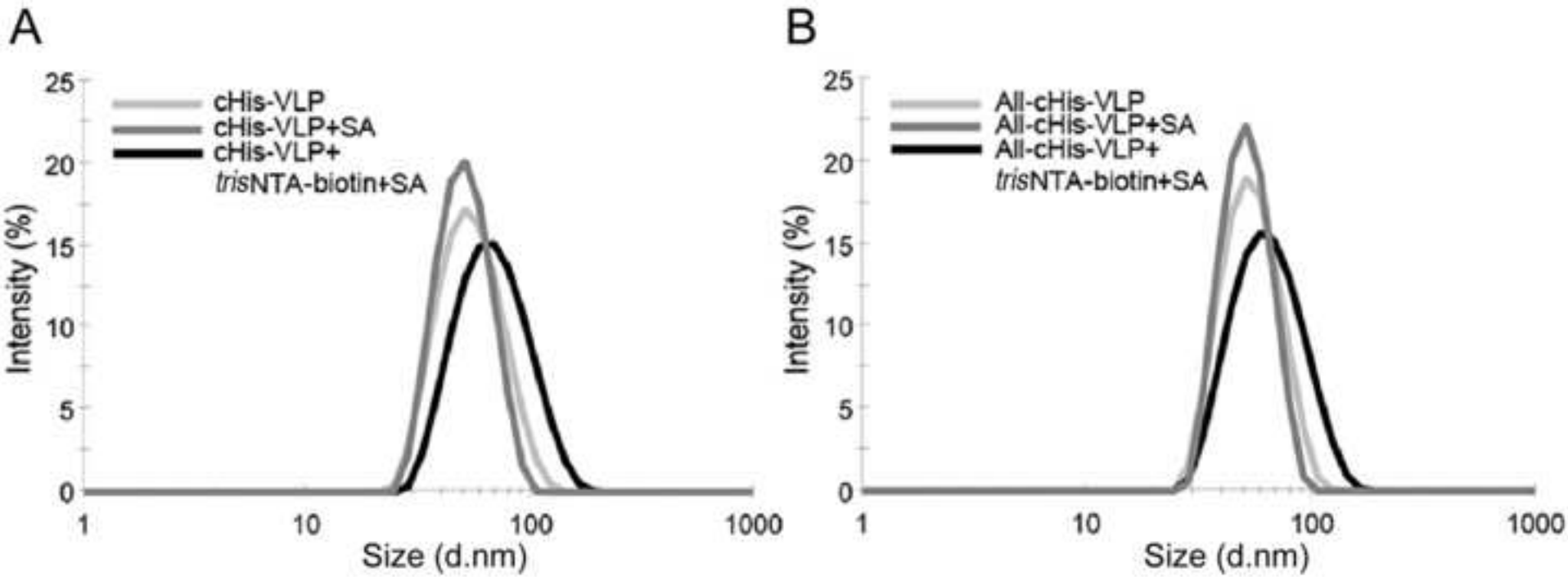

Figure 5

Click here to download high resolution image

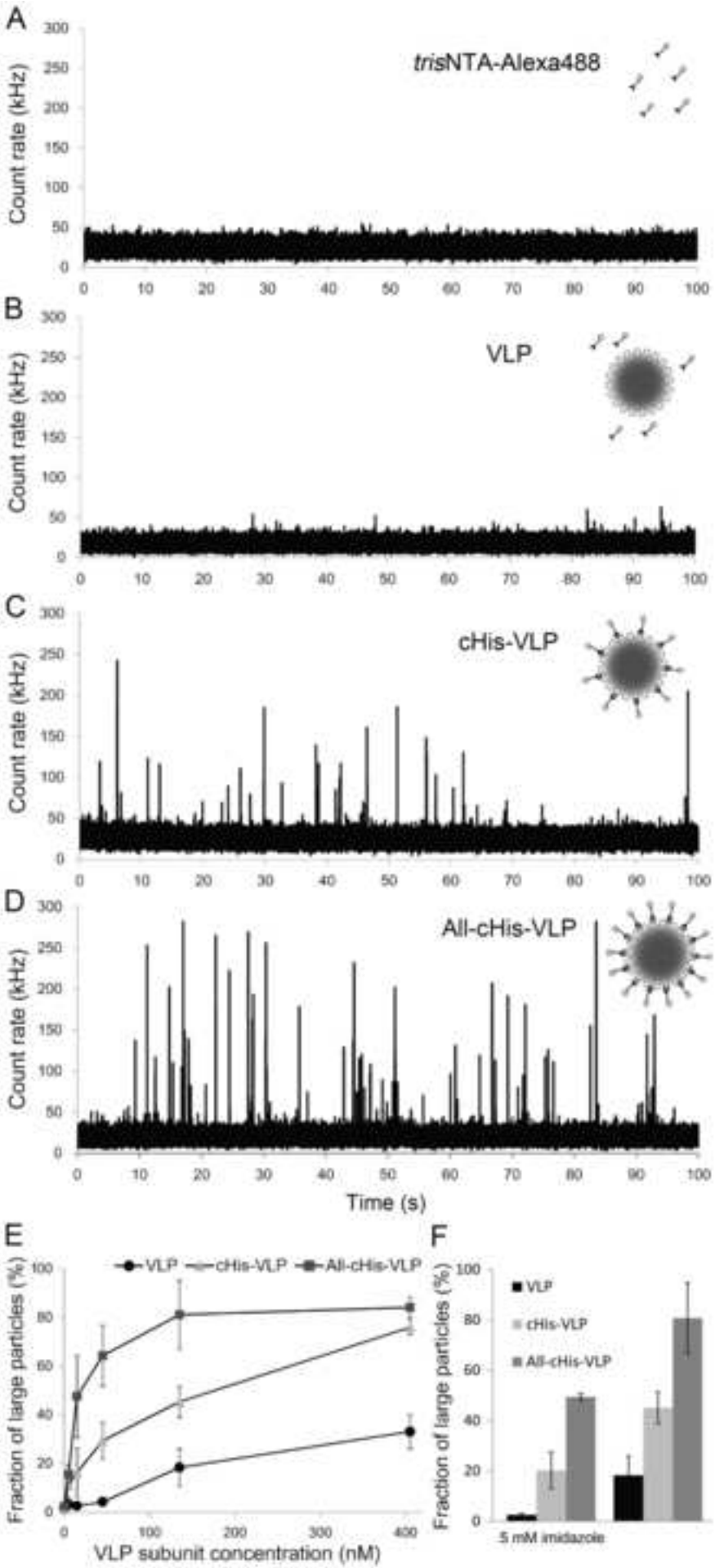

Figure 6

Click here to download high resolution image

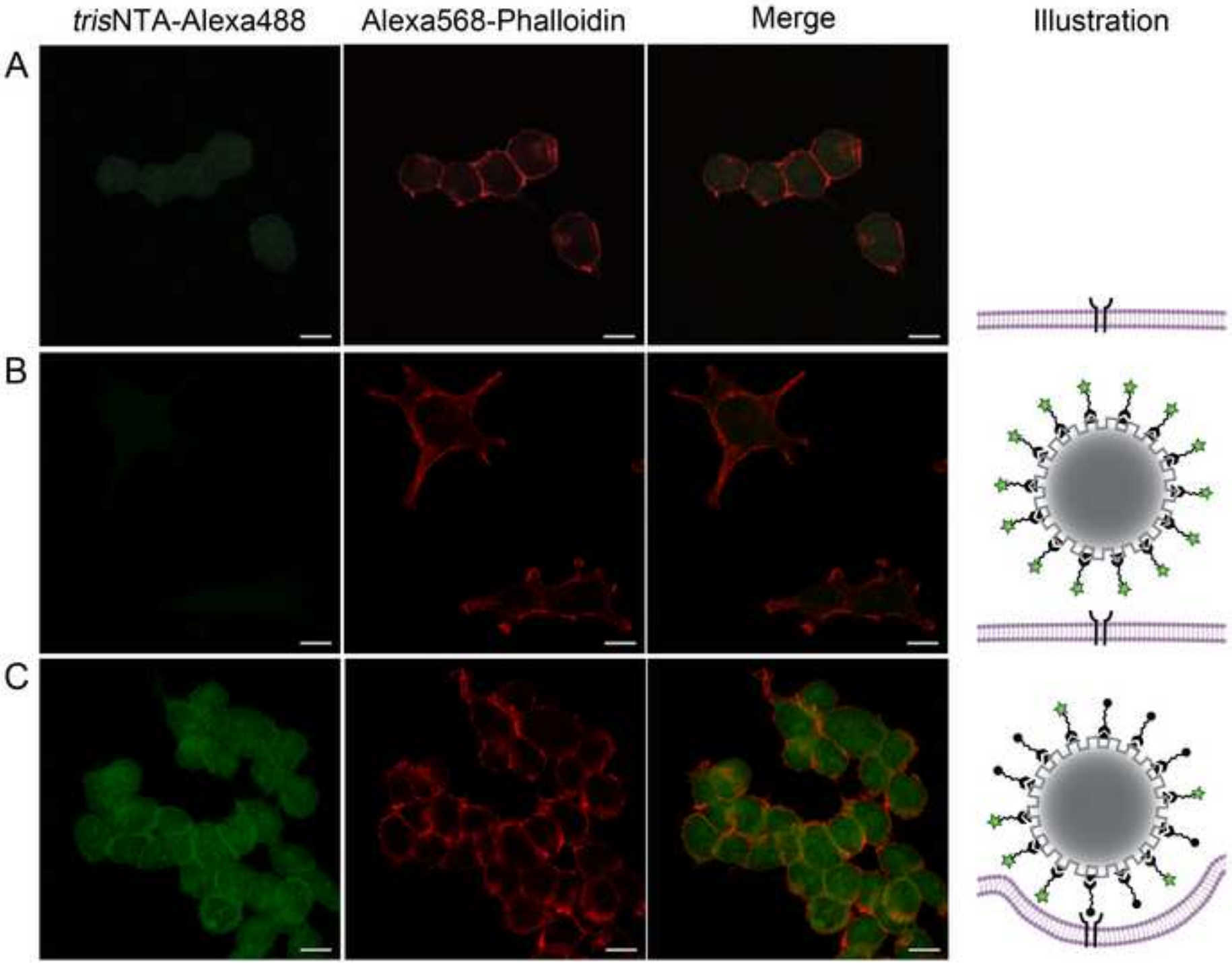

Supplementary material

Click here to download Supplementary material: Supplementary material_01072015.pdf